Redox Biology 46 (2021) 102130

Contents lists available at ScienceDirect

Redox Biology

journal homepage: www.elsevier.com/locate/redox

Identification of peroxiredoxin 6 as a direct target of withangulatin A by quantitative chemical proteomics in non-small cell lung cancer

Chen Chen [1], Lijie Gong [1], Xiaoqin Liu, Tianyu Zhu, Wuxi Zhou, Lingyi Kong [**], Jianguang Luo [*]

Jiangsu Key Laboratory of Bioactive Natural Product Research and State Key Laboratory of Natural Medicines, School of Traditional Chinese Pharmacy, China Pharmaceutical University, Nanjing, 210009, China

ARTICLE INFO

Keywords:
Peroxiredoxin 6
Oxidative stress
Withangulatin A
Covalent inhibitor
Non-small cell lung cancer

ABSTRACT

Peroxiredoxin 6 (PRDX6), as a bifunctional enzyme with glutathione peroxidase activity (GPx) and $Ca2^{+}$-independent phospholipase A2 (iPLA2) activity, has a higher expression in various cancer cells, which leads to the increase of antioxidant properties and promotes tumorigenesis. However, only a few inhibitors of PRDX6 have been discovered to date, especially the covalent inhibitors of PRDX6. Here, we firstly identified Withangulatin A (WA), a natural small molecule, as a novel covalent inhibitor of PRDX6. SILAC-ABPP identified that WA could directly bind to PRDX6 and inactivate the enzyme activity of PRDX6 by the α, β-unsaturated ketone moiety. Moreover, WA also facilitated the generation of ROS, and inhibited the GPx and iPLA2 activities. However, WA-1, with a reduced α, β-unsaturated ketone moiety, had no significant inhibition of the GPx and iPLA2 activities. Biolayer interferometry and LC-MS/MS analysis further demonstrated the selectively covalent binding of WA to the cysteine 47 residue (Cys47) of PRDX6, while mutation of Cys47 blocked the binding of WA to PRDX6. Notably, WA-mediated cytotoxicity and inhibition of the GPx and iPLA2 activities were almost abolished by the deficiency of PRDX6. Therefore, this study indicates that WA is a novel PRDX6 covalent inhibitor, which could covalently bind to the Cys47 of PRDX6 and holds great potential in developing anti-tumor agents for targeting PRDX6.

1. Introduction

The peroxiredoxins (PRDXs) are a ubiquitous family of highly conserved enzymes that use the thiol groups of their redox-active cysteines (Cys) to catalyze the reduction of peroxides, including hydrogen peroxide or other hydroperoxides [1–3]. The PRDXs are classified into two categories, 1-Cys and 2-Cys, based on whether the protein contains one or two conserved cysteine residues directly involved in catalysis [4–6]. There are six isoforms of PRDX enzymes (PRDX1-6) that have been identified in mammals to date [4]. In the PRDXs family, five (PRDX1, PRDX2, PRDX3, PRDX4, and PRDX5) are 2-Cys enzymes that utilize thioredoxin as the electron donor of their catalytic cycle [7]. Whereas PRDX6, the sole mammalian 1-Cys PRDX, uses glutathione (GSH) plus GSH S-transferase (GST) for reduction and resolution of its oxidized peroxidation Cys [2].

As the only 1-Cys PRDX, PRDX6 also has several significant functions that differ from the other PRDXs. Uniquely among the PRDXs, PRDX6 is the only peroxiredoxin that can bind and reduce phospholipid hydroperoxides (PLOOH) following oxidative stress, which is associated with a decreased content of phospholipid hydroperoxides in the cell membrane [6,8,9]. The activity responsible for PLOOH reduction of PRDX6 has been called phospholipid hydroperoxide GSH peroxidase (GPx) activity, which is similar to the enzymatic activity of GSH peroxidase 4 (GPX4) [10]. The GPx activity is thought to be of a major importance in the ability of PRDX6 to protect cells against oxidant stress [11]. Besides, unlike the other PRDXs, PRDX6 has a calcium-independent phospholipase A2 (iPLA2) activity [12]. The PLA2 activity catalyzes the hydrolysis of the acyl group at the sn-2 position of glycerophospholipids, with special affinity for phosphatidylcholines, to produce free fatty acids and a lysophospholipid [10]. Due to the various physiological and pathological functions, PRDX6 has been identified as a promising therapeutic target.

An increasing number of studies showed that the expression of PRDX6 is elevated in a variety of human cancers, including breast

* Corresponding author.
** Corresponding author.
E-mail addresses: cpu_lykong@126.com (L. Kong), luojg@cpu.edu.cn (J. Luo).
[1] These authors contributed equally to this work.

https://doi.org/10.1016/j.redox.2021.102130
Received 31 July 2021; Received in revised form 5 September 2021; Accepted 7 September 2021
Available online 9 September 2021

cancer, liver cancer, cervical cancer, ovarian cancer and lung cancer [13–17]. With the antioxidant properties, upregulation of PRDX6 facilitated the proliferation and development of cancers by protecting cancer cells against oxidative stress [7,18,19]. There had been reported that the GPx and iPLA2 activities were increased in cancer cells with high expression of PRDX6 [14,19,20]. Moreover, there have been reported that overexpressed PRDX6 could facilitate resistance to radiation and chemotherapeutics, while the inhibition of PRDX6 can sensitize cells to chemotherapy and promote apoptosis [16,21,22]. Conversely, the deficiency or downregulation of PRDX6 promoted the cell cycle arrest and apoptosis of cancer cells [17,23]. Thus, targeted inhibition of PRDX6 provides a potential therapeutic strategy for cancers with high expression of PRDX6. Nonetheless, only a few inhibitors of PRDX6 have been discovered to date. Therefore, it is of vital importance to discover the PRDX6 targeting inhibitors.

Withangulatin A (WA), a withanolide isolated from *Physalis angulata* var. *villosa*, has been reported to inhibit the proliferation of various cancer cells [24]. Herein, we first report that WA, a natural small molecule, is a novel covalent inhibitor of PRDX6. There had been reported that PRDX6 was highly expressed in non-small cell lung cancer cells, and overexpression of PRDX6 could significantly promote the proliferation of non-small cell lung cancer cells [14,19]. In this study, we found that WA remarkably inhibited the proliferation of H1975 non-small cell lung cancer cells, and identified that PRDX6 was the cellular target of WA by quantitative chemical proteomics. Further studies demonstrated that WA significantly suppressed the enzyme activity of PRDX6, and significantly inhibited the GPx and iPLA2 activities of H1975 cells. Unlike other competitive inhibitors, we demonstrated that WA selective covalently modified with the Cys47 residue (Cys47) of PRDX6 by the α, β-unsaturated ketone moiety and inactivated the PRDX6 to exhibit the inhibition of H1975 cells. These findings indicate that WA is a novel PRDX6 covalent inhibitor, which could be used as a promising lead compound in the development of PRDX6 inhibitor for oncotherapy.

2. Materials and methods

2.1. Compounds and cell lines

Withagulatin A (WA) was isolated from *Physalis angulata* var. *villosa* in our previous study [24]. NCI–H1975 (H1975) non-small cell lung cancer cells and human embryonic kidney 293T cells (HEK293T cells) were purchased from the Cell Bank of Shanghai Institute of Biochemistry and Cell Biology, Chinese Academy of Sciences (Shanghai, China). All cells were negative for Mycoplasma during this investigation. H1975 cells were cultured in RPMI-1640 (GIBCO, NY, USA) supplemented with 10% FBS (GIBCO, NY, USA) at 37 °C with 5% CO_2. HEK293T cells were cultured in DMEM (GIBCO, NY, USA) supplemented with 10% FBS (GIBCO, NY, USA) at 37 °C with 5% CO_2.

2.2. Cell viability and proliferation assay

The Cell Counting Kit-8 (CCK-8) assay which is used to test cell viability according to the manufacturer's protocol (MedChemExpress, NJ, USA). In brief, Cells (7×10^3/well) were seeded into a 96-well culture plate (Corning, NY, USA) for 24 h. Then cells were incubated with or without serial dilutions of WA for 24 h. Then the CCK-8 detection reagent was added and incubated for 4 h. The absorbance at 450 nm was measured by a microplate reader. For the colony formation assay, cells were seeded into 35 mm plates at a density of 1×10^3/well and incubated overnight. Then, the cells were treated with various concentrations of WA for 24 h. The growth medium was refreshed every three days. After 14 days, the cells were fixed and stained with a crystal violet solution (Sigma-Aldrich, MO, USA) for 15 min, and images of colonies were taken manually.

2.3. SILAC-ABPP and proteomics analysis of WA target proteins

The stable isotope labeling by amino acids in cell culture (SILAC) and activity-based protein profiling (ABPP) were based on previously reported procedures [25,26]. H1975 cells were grown in RPMI-1640 medium containing either Lysine and Arginine (Light) or $^{13}C_6$,$^{15}N_2$-Lysine and $^{13}C_6$,$^{15}N_4$-Arginine (Heavy). The "Light" or "Heavy" cells were preincubated with 20 μM of WA or DMSO for 2 h, and then treated with WP for 4 h. After incubation, the cells were lysed. Next 100 μM of Biotin-N_3 (from 100 mM stock solution in DMSO), 1 mM of CuSO4 (from 50 mM stock solution in deionized water), 100 μM of TBTA (from 100 mM stock solution in deionized water) and 1 mM of TECP (from 100 mM stock solution in deionized water) were added to the lysates. The reaction was further incubated for 2 h with gentle mixing at room temperature. Next, tagged proteins were precipitated with prechilled acetone. The precipitated proteins were subsequently collected by centrifugation (15000 rpm, 10 min, 4 °C). Then the precipitated proteins were redissolved with 200 μl of lysis buffer by sonication. Upon incubation with streptavidin beads for 2 h at room temperature, the beads were washed with PBS. The enriched proteins were suspended by 1 × loading buffer and boiled for 15 min, then separated by SDS-PAGE for target validation and analyzed by LC-MS/MS.

2.4. Drug affinity responsive target stability (DARTS)

DARTS was performed as previously reported [27]. Briefly, the cells were collected and total protein was isolated by using lysis buffer. The cell lysates were centrifuged at 15000 rpm for 15 min at 4 °C. The supernatants were 1:10 diluted with 10 × TNC buffer (500 mM Tris-HCl, pH 8.0, 500 mM NaCl, 100 mM $CaCl_2$) and treated with different concentrations of WA or DMSO. After incubation for 1 h at room temperature, pronase (5 μg/ml) was added into the lysates for a further 15 min at 37 °C. Reactions were stopped by adding protease inhibitor cocktail and SDS-PAGE loading buffer followed by immunoblotting.

2.5. Cellular thermal shift assay (CETSA)

CETSA was performed as previously reported [27]. Briefly, H1975 cells were treated with WA (4 μM) or DMSO and incubated for 4 h. Cells were collected and washed with PBS, then resuspended to a density of 5×10^6 cells/ml in PBS supplemented with protease inhibitor. 100 μl of each cell suspension was then dispensed into PCR tubes and heated at 44–60 °C by a thermal cycler for 3 min and immediately lysed by freeze-thaw in liquid nitrogen. The cell lysates were clarified by centrifugation at 15000 rpm for 15 min at 4 °C. Then supernatants were analyzed by immunoblotting.

2.6. Biolayer interferometry assay (BLI)

The binding affinities of compounds for recombinant PRDX6 or mutant recombinant PRDX6 were determined by a biolayer interferometry assay using Octet RED96 (ForteBio). Ni-NTA biosensor tips (ForteBio, Menlo Park, CA) were used to immobilize the his-labeled proteins after prewetting with kinetic buffer (PBS, 0.05% bovine serum albumin, 0.01% Tween 20). The equilibrated Ni-NTA biosensors were loaded with recombinant proteins (100 μg/ml). Background binding controls used a duplicate set of sensors that incubated in a buffer without proteins. All assays were performed by a standard protocol in 96-well black plates with a total volume of 250 μl/well at 30 °C. All the data were analyzed by Octet data analysis software. The signals were analyzed by a double reference subtraction protocol to deduce nonspecific and background signals and signal drifts caused by biosensor variability. Equilibrium dissociation constant (K_D) values were calculated from the ratio of K_{off} to K_{on}.

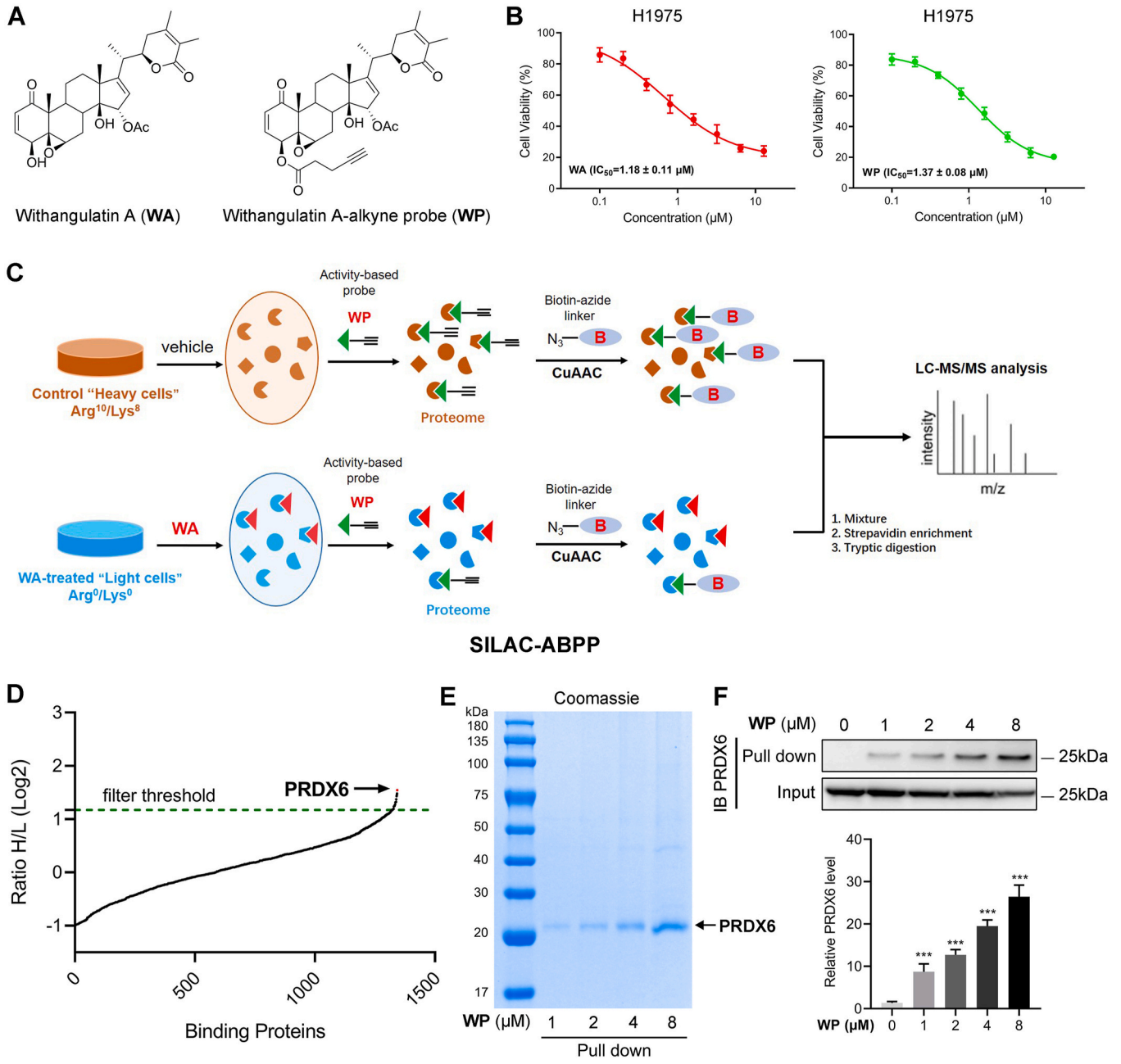

Fig. 1. The quantitative chemical proteomics identified PRDX6 as the direct target of Withangulatin A. (A) Chemical structures of Withangulatin A (WA) and Withangulatin A-alkyne probe (WP). (B) The cell viabilities of H1975 cells treated by WA and WP were measured by CCK-8 assay. (C) The overall scheme of the SILAC-ABPP (stable isotope labeling by amino acids in cell culture-activity-based protein profiling) experiments to profile WA targets in situ. (D) The SILAC Heavy/Light (H/L) ratio was measured by a competitive SILAC assay. (E) Labeling of recombinant PRDX6 protein with different concentrations of WP. Protein affinity pull-down assay was performed and the precipitated proteins were processed by coomassie blue staining. (F) Protein affinity pull-down assay was performed in H1975 cells by different concentrations of WP, and immunoblotting by PRDX6 antibody. Data are presented as the mean ± SD, n = 3, $^{***}P < 0.001$, compared with control group (0 μM). (For interpretation of the references to colour in this figure legend, the reader is referred to the Web version of this article.)

2.7. The PRDX6 enzyme assay

PRDX6 enzyme activity was determined as previously reported [28]. Briefly, the reaction buffer was 50 mM Tris-HC1 (pH 8.0), 0.1 mM EDTA, 0.3 mM NADPH, 0.36 mM GSH, and 0.23 units/ml glutathione reductase. For the inhibition assay, compounds and recombinant Prdx6 were preincubated at room temperature for 30 min. Fluorescence was continuously recorded at 460 nm (340 nm excitation). After a steady baseline was achieved, the reaction was started by the addition of substrate (7.6 μM H_2O_2 or 100 μM PLPCOOH plus 0.1% Triton X-100) and the linear change in fluorescence indicating utilization of NADPH for reduction of oxidized GSH.

2.8. GPx activity and iPLA2 activity assay

Intracellular GPx activity and iPLA2 activity were performed as previously reported [19,20]. Briefly, GPx assay and iPLA2 assay kits were purchased from Cayman Chemical (703102, 765021, MI, USA), and the activities were measured according to the manufacturer's recommendations.

2.9. Generation of PRDX6 knockout (KO) cell lines by CRISPR/Cas9 system

To obtain the PRDX6 KO H1975 cells, H1975 cells were transfected with the PRDX 6 CRISPR/Cas9 KO plasmid according to the manufacturer's instructions (sc-401549-HDR, Santa Cruz Biotechnology, Inc.). After transfection, cells were selected with puromycin according to the manufacturer's instructions, then single clones were picked and validated by immunoblotting analysis.

2.10. Measurement of reactive oxygen species (ROS) levels

The intracellular ROS levels were measured as previously described [29]. Briefly, the H1975 cells were incubated with serial dilutions of WA for 12 h. Then incubated in the dark with 10 mM oxidation-sensitive fluorescent probe DCFH-DA (Beyotime Biotechnology, China) for 20 min at 37 °C. The fluorescence intensity was then measured with a BD Accuri C6 flow cytometer or an imageXpress® confocal microscope.

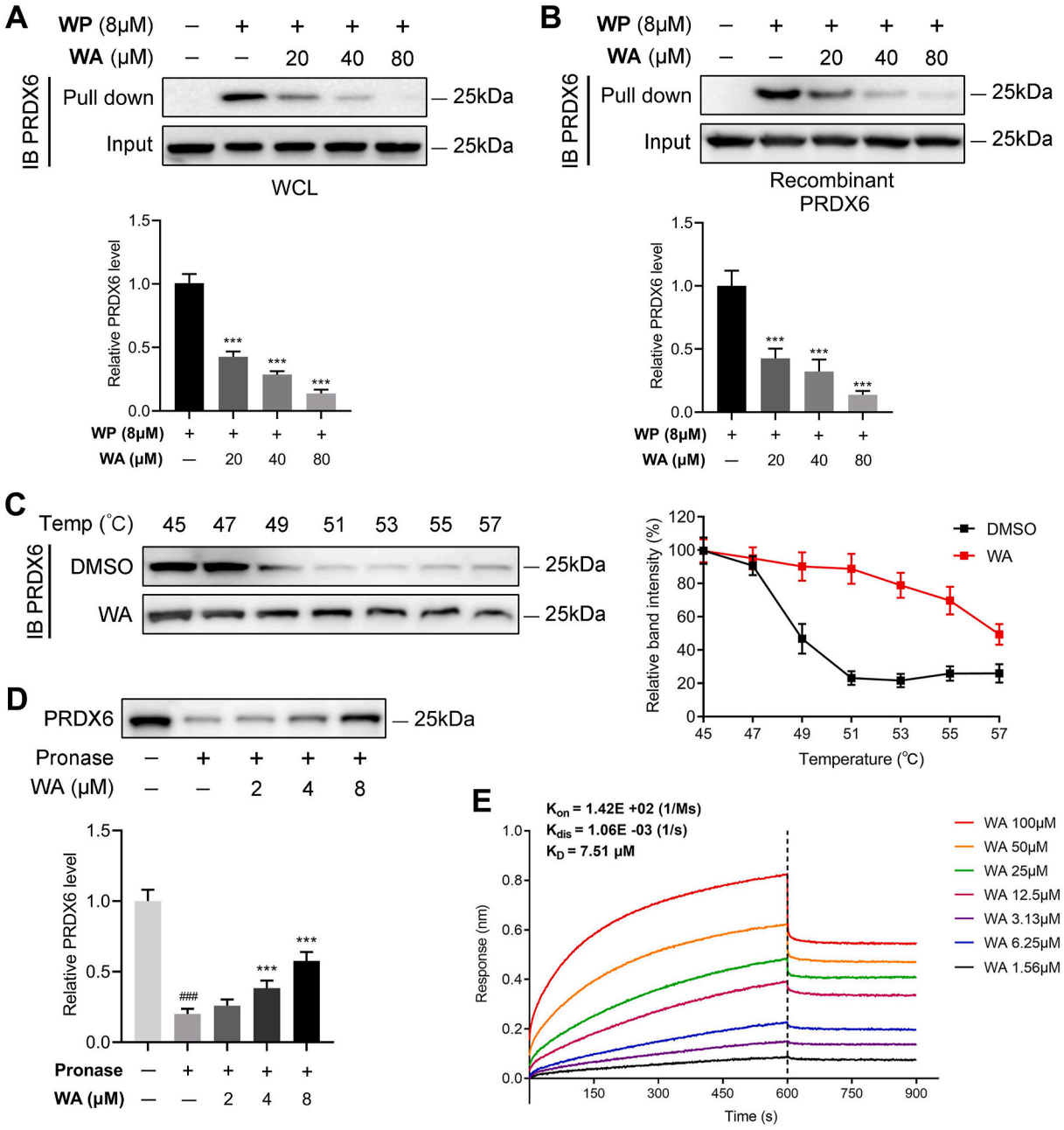

Fig. 2. WA directly binds to PRDX6. (A) Immunoblotting analysis of the whole cell lysate (WCL) in H1975 cells or (B) the recombinant PRDX6 protein treated with WP in the absence or presence of WA for the competitive binding, and followed by protein affinity pull-down assay. The PRDX6 bound to the WP was detected by immunoblotting. Data are presented as the mean ± SD, n = 3, $^{***}P < 0.001$, compared with WP alone group (8 μM). (C) The CETSA assay was used to evaluate the binding between WA (4 μM) and PRDX6 in thermodynamic levels. The expression of PRDX6 was detected by immunoblotting. (D) H1975 cells lysates were treated with different concentrations of WA, and then incubated with pronase (5 μg/ml). The expression of PRDX6 was detected by immunoblotting. Data are presented as the mean ± SD, n = 3, $^{\#\#\#}P < 0.001$, compared with lysates group, $^{***}P < 0.001$, compared with pronase alone group. (E) Interaction between WA and recombinant PRDX6 protein was analyzed by BLI assay.

2.11. Measurement of total antioxidant capacity (T-AOC), 4-hydroxynonenal (4-HNE) and malondialdehyde (MDA) levels

The T-AOC, 4-HNE and MDA levels were measured as previously described [30,31]. Briefly, the T-AOC levels were measured by using the total antioxidant assay kit (Beyotime Biotechnology, China). The detailed measurements were carried out with reference of the kit instructions. The 4-HNE concentrations were examined by an Elisa assay kit (Elabscience, China). The detailed measurements were carried out according to the manufacturer's instructions. The MDA concentrations were measured using a Lipid Peroxidation MDA assay kit (Beyotime Biotechnology, China). The detailed measurements were carried out with reference of the kit instructions.

2.12. Plasmid transfection

The PRDX6 C47A plasmid was purchased from Zoonbio Biotechnology (Nanjing, China). Cells were seeded in 6-well plates. The PRDX6 C47A plasmid were transfected into the cells using Lipofectamine 3000 (Invitrogen, Carlsbad, CA) according to the manufacturer's instructions. The primer sequence was showed in Supplementary Table 2.

2.13. Immunoblotting analysis

Cells with different treatments were washed twice with PBS, then collected and lysed in RIPA buffer. The cell lysates were separated on SDS polyacrylamide gels and transferred to PVDF membranes (Bio-Rad, Hercules, CA). After blocking nonspecific binding with TBS-T (0.1% Tween) containing 5% non-fat milk for 1 h at room temperature, the membranes were immunoblotted with the primary antibodies at 4 °C overnight. Then, the membranes were incubated with HRP-conjugated goat anti-rabbit secondary antibody for 2 h at room temperature. The protein bands were detected using the ChemiDOC™ system (Bio-Rad, Hercules, CA).

2.14. Xenograft tumor model

Five-week-old male BALB/c nude mice were purchased from the Model Animal Research Center of Nanjing University (Nanjing, China). For the tumor xenograft assay, 3×10^6 H1975 cells were suspended in 200 μl PBS and subcutaneously injected into the right flank of the mice. When the tumors reached approximately 100 mm^3, the tumor-bearing mice were randomly divided into four groups. Then, WA (5 mg/kg or 10 mg/kg) were intraperitoneally administered every three days. After four weeks, all of the mice were euthanized. Then, the tumors and visceral organs of each group were collected and fixed in 4% paraformaldehyde. All animal experimental procedures followed the National Institutes of Health guide for the care and use of laboratory animals and were performed in accordance with protocols approved by the Institutional Animal Care and Use Committee (IACUC) of China Pharmaceutical University Experimental Animal Center.

2.15. Statistical analysis

Statistical significance was determined using GraphPad Prism Software 8. Data are represented as mean ± SD. Student's *t*-test and one-way ANOVA test were used for statistical analyses of the data. $P < 0.05$, <0.01 or <0.001 were considered statistically significant.

3. Results

3.1. PRDX6 is identified as a direct target of WA by SILAC-ABPP

To explore and identify the cellular targets of WA, an alkyne-tagged WA-based probe WP was designed and synthesized (Fig. 1A and Scheme S1). The alkyne tag can be further appended with an azide-biotin tag through click chemistry, allowing the cellular targets of WA to be affinity purified for mass spectrometry identification [32]. The cytotoxic experiment showed that WA significantly suppressed the proliferation of H1975 non-small cell lung cancer cells (Fig. 1B and Fig. S1). WP had similar cytotoxicity compared with WA (Fig. 1B), suggesting that the addition of the alkyne tag had no significant influence on the cytotoxic activity of WA.

Affinity-based protein profiling (ABPP), as a chemical proteomics strategy, is usually employed to identify the protein targets of bioactive small molecules [33,34]. Especially, the stable isotope labeling by amino acids in cell culture (SILAC), a widely used method in quantitative chemical proteomics, has been successfully performed by the combination of ABPP for target identification of bioactive small molecules [35]. Thus, we applied WP for identifying the cellular targets of WA through SILAC-ABPP experiments in situ (Fig. 1C). After competition by excessive WA and protein affinity pull-down assay, the digested peptides were analyzed by LC-MS/MS. The LC-MS/MS analysis indicated that the quantified SILAC ratio (heavy/light) of PRDX6 was the highest (Fig. 1D and Supplementary Table 1). Furthermore, the results of the coomassie blue assay and immunoblotting assay revealed that PRDX6 was pulled down by WP both in recombinant PRDX6 protein and H1975 cells (Fig. 1E and F). These data indicate that PRDX6 is a direct target of WA in H1975 cells.

Although the thioredoxin (TXN), thioredoxin reductase1 (TXNRD1), glutathione reductase (GSR) and other peroxiredoxins (PRDXs) were also identified, the quantified SILAC ratio of these proteins were less than that of PRDX6. Moreover, the significance B of the quantified SILAC ratio of these proteins (TXN, TXNRD1, GSR and PRDXs) were>0.05 (Supplementary Table 1), indicating the interactions of WA with TXN, TXNRD1, GSR and PRDXs had no significant difference. As shown in Fig. S2, WA had no significant effect on the activities of TXN, TXNRD and GSR in H1975 cells at the corresponding concentration (0.25–1 μM), which was consistent with our previous study [36]. Furthermore, we also examined the difference of the binding capacities of WA with PRDXs. As shown in Fig. S3, the protein affinity pull-down assay showed that the binding between WP and PRDX6 was the strongest among the PRDXs under the same condition. Therefore, we considered that PRDX6 was a major target protein of WA.

3.2. WA directly binds to PRDX6

To further validate the interaction of WA with PRDX6, we carried out competitive binding experiments by excessive WA. Notably, the binding of WP to PRDX6 was blocked by preincubating with WA both in H1975 cells and recombinant PRDX6 protein (Fig. 2A and B). We next performed the CETSA and DARTS assays in H1975 cells. The CETSA assay is used to examine the interaction between the protein and compound, while the thermal stability of protein is elevated after the compound bound to protein [27]. The DARTS assay is also applied to test the interaction between the protein and compound, while the binding of compound to protein could against the proteolysis by pronase [27]. The thermal stability of PRDX6 was increased after the treatment of WA in CETSA, suggesting the interaction of WA with PRDX6 (Fig. 2C). Meanwhile, WA also significantly reversed the proteolysis of PRDX6 by pronase, suggesting WA could bind to PRDX6 (Fig. 2D). More importantly, the BLI assay further confirmed that there was a strong direct interaction between WA and PRDX6, and the K_D value of WA binding to recombinant PRDX6 protein was 7.51 μM (Fig. 2E). Collectively, these results indicate that WA could directly bind to PRDX6.

3.3. WA covalently binds to PRDX6 by the α, β-unsaturated ketone moiety

We further investigated whether WA could irreversibly bind to PRDX6. Interestingly, posttreatment with excessive WA could not prevent PRDX6 binding to WP both in H1975 cells and recombinant PRDX6

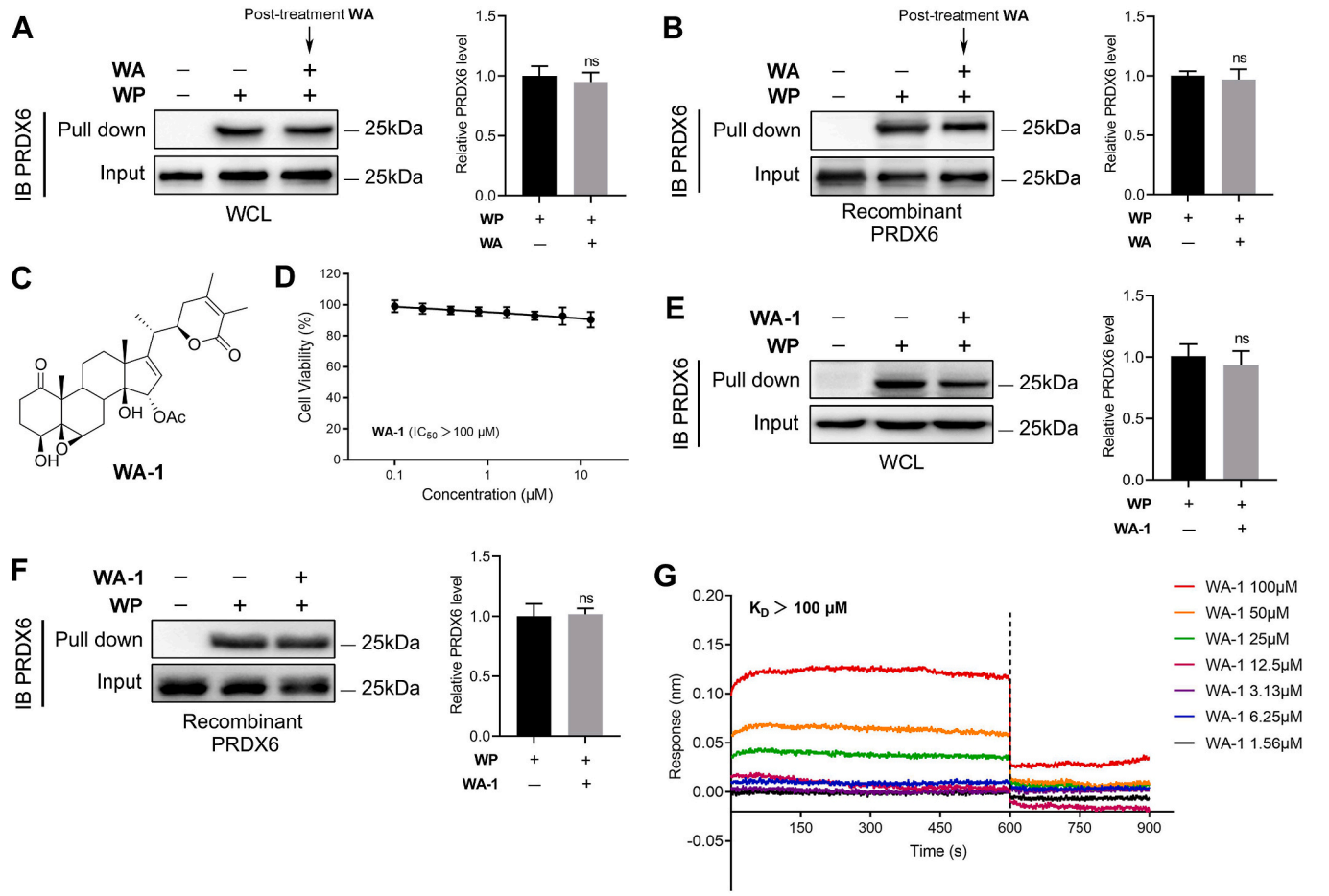

Fig. 3. WA irreversibly binds to PRDX6. (A) H1975 cells were preincubated with WP (4 μM) for 4 h and further incubated with or without WA (40 μM) for 2 h, then protein affinity pull-down assay was performed. Data are presented as the mean ± SD, n = 3, ns, no significance, compared with WP alone group. (B) The recombinant PRDX6 protein was preincubated with WP (4 μM) for 2 h and further incubated with or without WA (40 μM) for 2 h, then protein affinity pull-down assay was performed. Data are presented as the mean ± SD, n = 3, ns, no significance, compared with WP alone group. (C) Chemical structures of WA analog WA-1 (with the reduced α,β-unsaturated ketone moiety). (D) The cell viability of H1975 cells treated by WA-1 was measured by a CCK-8 assay. (E) H1975 cells were preincubated with or without WA-1 (40 μM) for 2 h and further incubated with WP (4 μM) for 4 h, then protein affinity pull-down assay was performed. Data are presented as the mean ± SD, n = 3, ns, no significance, compared with WP alone group. (F) The recombinant PRDX6 protein was preincubated with or without WA-1 (40 μM) for 2 h and further incubated with WP (4 μM) for 2 h, then protein affinity pull-down assay was performed. Data are presented as the mean ± SD, n = 3, ns, no significance, compared with WP alone group. (G) Interaction between WA-1 and recombinant PRDX6 protein was analyzed by BLI assay.

protein (Fig. 3A and B), revealing the existence of an irreversible interaction between WA and PRDX6. Due to the α, β-unsaturated ketone moiety is considered as a Michael acceptor that could covalently bind to the thiol of cysteine in protein, which is essential for the biological activity of multiple compounds [37,38]. We speculated whether WA is reacted with PRDX6 by the α, β-unsaturated ketone moiety. Therefore, we synthesized WA-1 by reduction reaction of WA to reduce the α, β-unsaturated ketone moiety (Fig. 3C and Scheme S2). Strikingly, WA-1 had no obvious influence on the proliferation of H1975 cells (Fig. 3D), suggesting that the cytotoxicity of WA depended on the α, β-unsaturated ketone moiety. Meanwhile, it was noteworthy that preincubation of WA-1 could not prevent PRDX6 binding to WP both in H1975 cells and recombinant PRDX6 protein (Fig. 3E and F), further indicating that WA covalently bound to PRDX6 by the α, β-unsaturated ketone moiety. BLI assay further confirmed that there was no obvious direct interaction between WA-1 and PRDX6, which the K_D value of WA-1 binding to recombinant PRDX6 protein was more than 100 μM (Fig. 3G). Taken together, these results indicate that WA could covalently bind to PRDX6.

3.4. Cysteine 47 residue of PRDX6 is covalently modified by WA

Since the α, β-unsaturated ketone moiety of WA is most likely a reactive Michael acceptor, which might form a covalent bond with cysteine residues of proteins. Therefore, we speculated that the cysteine residues in PRDX6 (Fig. S4) might be the binding sites of WA. To confirm which of these residues was modified by WA, we incubated recombinant PRDX6 protein with or without WA followed by LC-MS/MS analysis. In our previous study, we found that WA could break into fragments during the LC-MS/MS analysis, which the MS/MS spectra of WA showed sodiated ion at *m/z* 489.2255, which might be obtained via neutral losses of CH_3COOH (Fig. S5). Thus, we performed the protein MS/MS database search by using the mass of 466.24 Da. The further MS/MS analysis proved that the Cys47-containing peptide DFTPVC$_{47}$TTELGR (from y7 to y9 fragment ions) had a 466.24 Da mass shift in the peptide spectra of the WA treatment group (Fig. 4A and B), which was consistent with the addition of one molecular unit of WA-residue (466.24 Da).

In PRDX1-5 (2-cys peroxiredoxins, Supplementary Table 3), the resulting sulfenic acid then reacts with another (resolving) cysteine residue, forming a disulfide that is subsequently reduced by an appropriate electron donor to complete a catalytic cycle [7]. PRDX6 also contains another cysteine residue (Cys91), which is not the active-site Cys residue of PRDX6. However, we did not find the binding of WA to the Cys91 of PRDX6 in the LC-MS/MS analysis (Fig. S6).

To further prove the binding of WA to the Cys47 of PRDX6, we

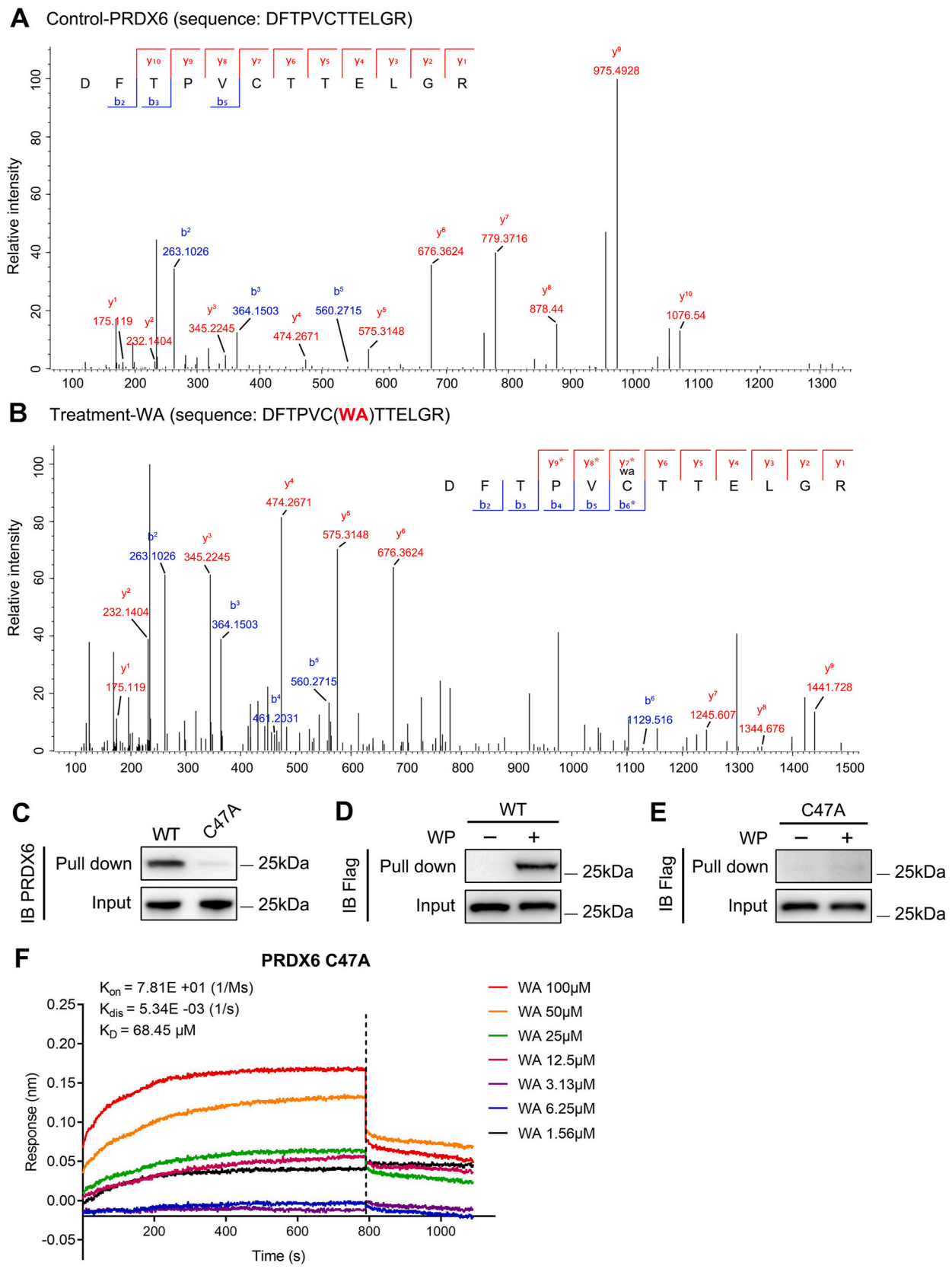

Fig. 4. WA selective covalently binds to the Cys47 residue of PRDX6. (A) The recombinant PRDX6 protein was incubated without or (B) with WA, then the peptide fragment were identified by MS/MS. (C) The recombinant WT PRDX6 and mutant PRDX6 (C47A) proteins were incubated with WP, and followed by protein affinity pull-down assay. The PRDX6 bound to the WP was detected by immunoblotting. (D) Flag-tagged PRDX6 and mutant (E) PRDX6 C47A were expressed in HEK-293T cells. The protein affinity pull-down assay was performed by WP. The expression of Flag-PRDX6 was detected by immunoblotting. (F) BLI analysis of the interaction between WA and recombinant PRDX6 C47A protein.

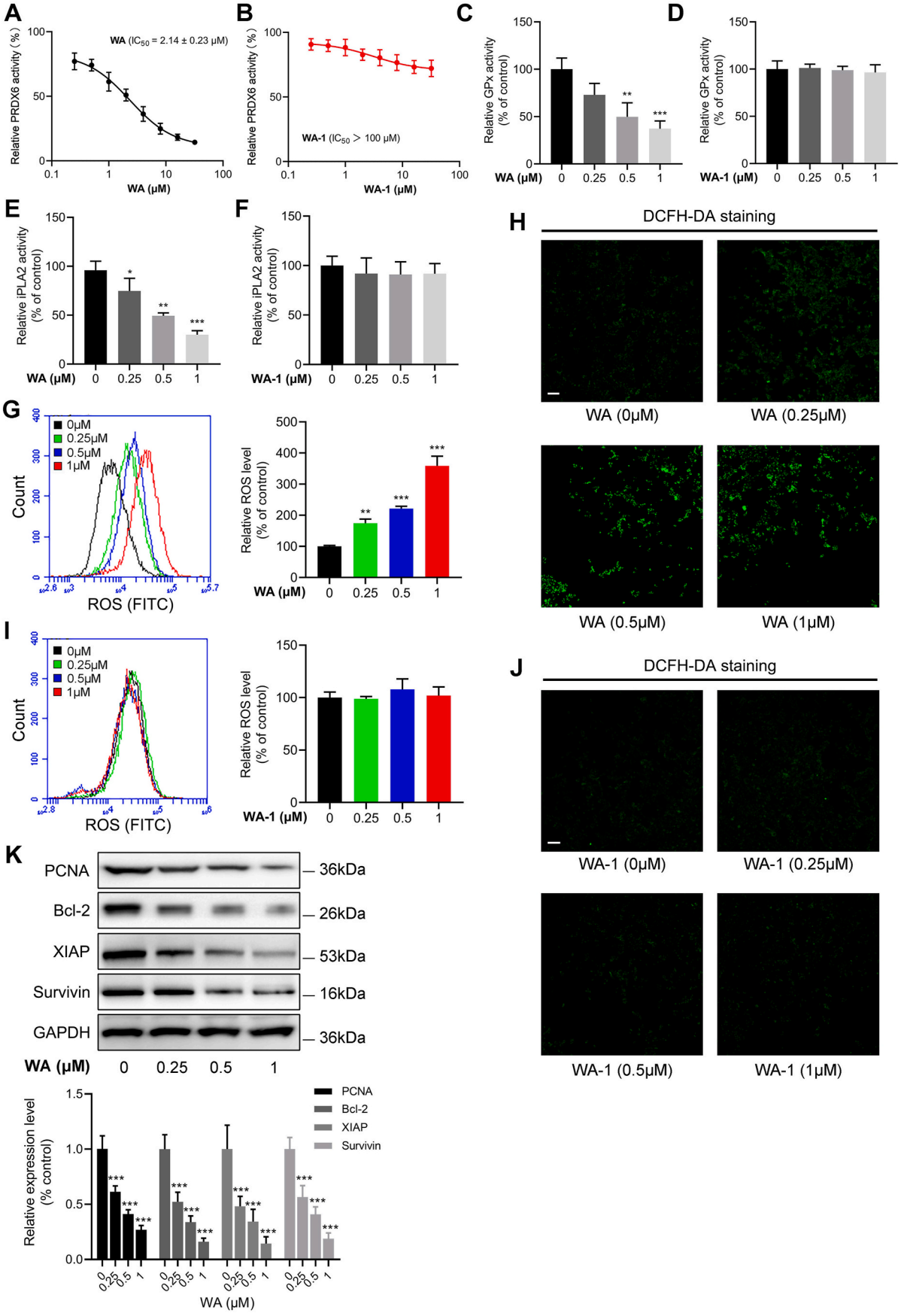

(caption on next page)

Fig. 5. WA inhibits the activity of PRDX6 and promotes the generation of ROS. (A) Dose-response inhibition curve of PRDX6 enzyme activity by WA and (B) WA-1 were measured by PRDX6 enzyme assay. (C) H1975 cells were treated with different concentrations of WA or (D) WA-1 for 12 h, then the GPx activities were measured by a GPx assay kit. Data are presented as the mean ± SD, n = 3, $^{**}P < 0.01$, $^{***}P < 0.001$, compared with control group (0 μM). (E) H1975 cells were treated with different concentrations of WA or (F) WA-1 for 12 h, then the iPLA2 activities were measured by an iPLA2 assay kit. Data are presented as the mean ± SD, n = 3, $^{*}P < 0.05$, $^{**}P < 0.01$, $^{***}P < 0.001$, compared with control group (0 μM). (G) H1975 cells were treated with different concentrations of WA for 12 h, then the ROS levels in H1975 cells were measured by flow cytometry and (H) fluorescence microscope (DCFH-DA staining). Data are presented as the mean ± SD, n = 3, $^{**}P < 0.01$, $^{***}P < 0.001$, compared with control group (0 μM). Scale bar = 50 μm. (I) H1975 cells were treated with different concentrations of WA-1 for 12 h, then the ROS levels in H1975 cells were measured by flow cytometry and (J) fluorescence microscope. Scale bar = 50 μm. (K) The expression of PCNA, Bcl-2, XIAP and survivin in H1975 cells were measured by immunoblotting after treatment with different concentrations of WA for 24 h. Data are presented as the mean ± SD, n = 3, $^{***}P < 0.001$, compared with control group (0 μM).

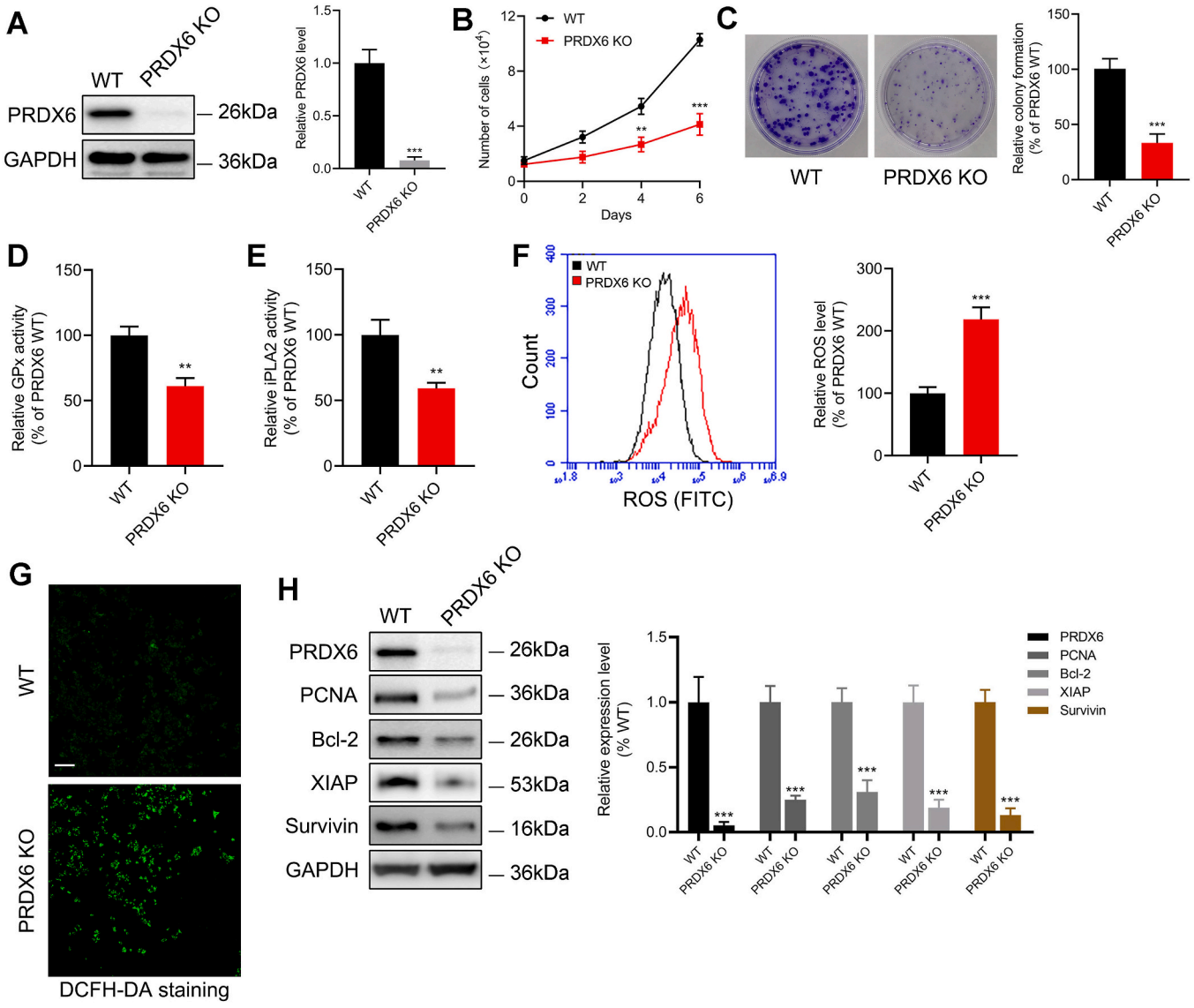

Fig. 6. Effect of PRDX6 knockout (KO) on the proliferation and oxidative stress of H1975 cells. (A) Immunoblotting analysis of the PRDX6 in WT and PRDX6 KO H1975 cells by the CRISPR/Cas9 system. Data are presented as the mean ± SD, n = 3, $^{***}P < 0.001$, compared with WT group. (B) Growth curve of WT and PRDX6 KO H1975 cells. Data are presented as the mean ± SD, n = 6, $^{***}P < 0.001$, compared with WT group. (C) Cell proliferative activity of PRDX6 WT and PRDX6 KO H1975 cells were evaluated by the colony formation assay. Data are presented as the mean ± SD, n = 3, $^{***}P < 0.001$, compared with WT group. (D) GPx activities and (E) iPLA2 activities of PRDX6 WT and PRDX6 KO H1975 cells were measured by a GPx assay kit or an iPLA2 assay kit. Data are presented as the mean ± SD, n = 3, $^{**}P < 0.01$, compared with WT group. (F) The ROS levels of PRDX6 WT and PRDX6 KO H1975 cells were measured by flow cytometry. Data are presented as the mean ± SD, n = 3, $^{***}P < 0.001$, compared with WT group. (G) The ROS levels of PRDX6 WT and PRDX6 KO H1975 cells were measured by fluorescence microscope. Scale bar = 50 μm. (H) The expression of PCNA, Bcl-2, XIAP and survivin in PRDX6 KO H1975 cells were measured by immunoblotting. Data are presented as the mean ± SD, n = 3, $^{***}P < 0.001$, compared with WT group.

mutated Cys47 of PRDX6 into alanine. The protein affinity pull-down assay further demonstrated that the C47A mutation abolished the capacity of PRDX6 binding to WP (Fig. 4C). In vivo, we also transfected Flag-PRDX6 and C47A mutated Flag-PRDX6 plasmid into HEK293T cells which is usually used for transfection and protein expression, and followed by a protein affinity pull-down assay with WP. Immunoblotting

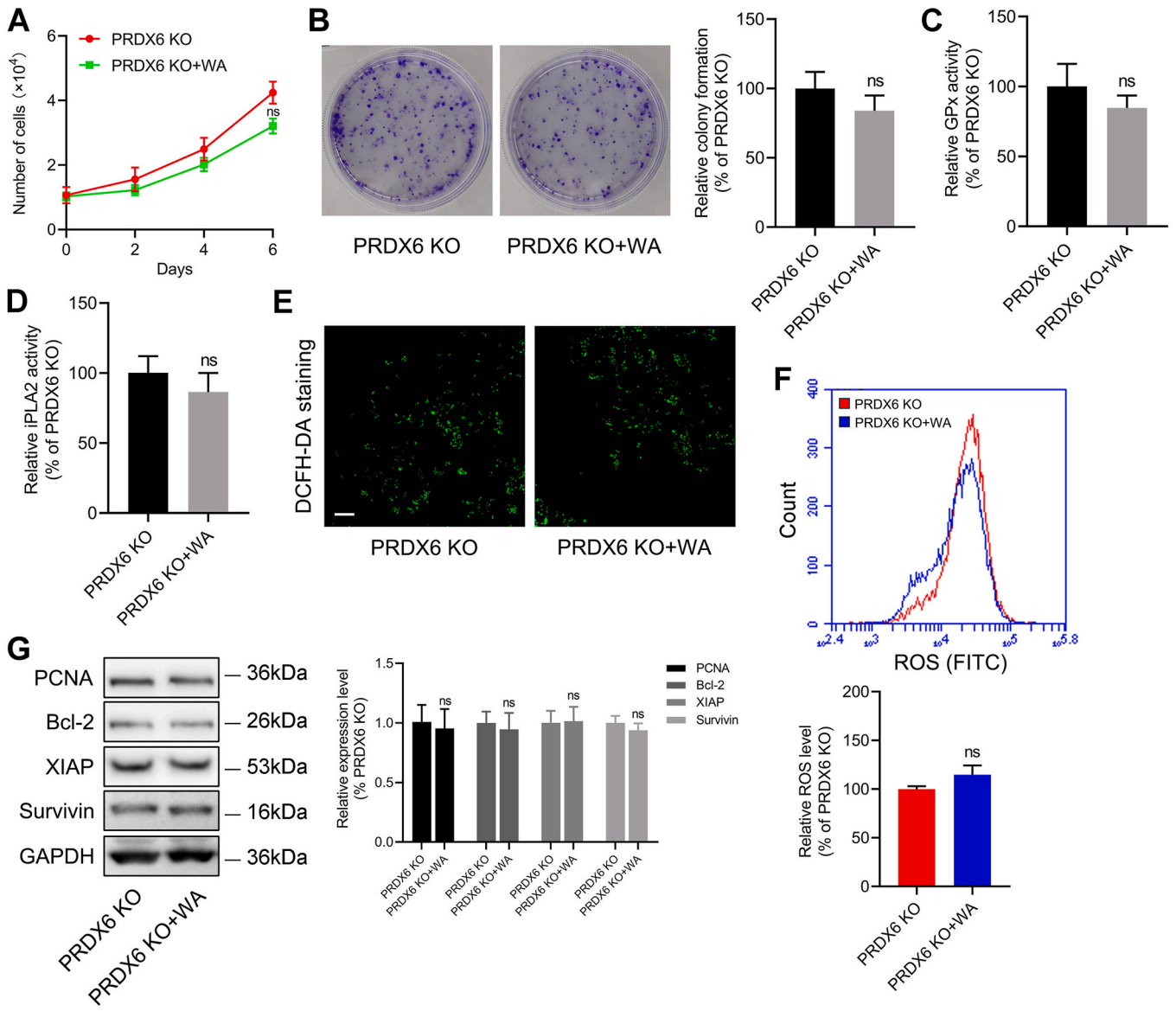

Fig. 7. Effect of WA on the proliferation and oxidative stress of PRDX6 KO H1975 cells. (A) Growth curves of PRDX6 KO H1975 cells after treatment with or without WA (1 μM). Data are presented as the mean ± SD, n = 6, ns, no significance, compared with PRDX6 KO group. (B) Cell proliferative activity of PRDX6 KO H1975 cells after treatment with or without WA (1 μM) by the colony formation assay. Data are presented as the mean ± SD, n = 3, ns, no significance, compared with PRDX6 KO group. (C) PRDX6 KO H1975 cells were treated with or without WA (1 μM) for 12 h, then the GPx activities were measured by a GPx assay kit. Data are presented as the mean ± SD, n = 3, ns, no significance, compared with PRDX6 KO group. (D) PRDX6 KO H1975 cells were treated with or without WA (1 μM) for 12 h, then the iPLA2 activities were measured by an iPLA2 assay kit. Data are presented as the mean ± SD, n = 3, ns, no significance, compared with PRDX6 KO group. (E) PRDX6 KO H1975 cells were treated with or without WA (1 μM) for 12 h, then the ROS levels were measured by fluorescence microscope. Scale bar = 50 μm. (F) PRDX6 KO H1975 cells were treated with or without WA (1 μM) for 12 h, then the ROS levels were measured by flow cytometry. Data are presented as the mean ± SD, n = 3, ns, no significance, compared with PRDX6 KO group. (G) The expression of PCNA, Bcl-2, XIAP and survivin in PRDX6 KO H1975 cells were measured by immunoblotting after treatment with WA (1 μM) for 24 h. Data are presented as the mean ± SD, n = 3, ns, no significance, compared with PRDX6 KO group.

results revealed that Flag-PRDX6 could bind to WP, while C47A mutated Flag-PRDX6 was not bound to WP (Fig. 4D and E). What's more, the BLI assay further certified that there was a weak interaction between WA and recombinant PRDX6 C47A proteins, which the K_D value of WA binding to recombinant PRDX6 C47A proteins was 68.45 μM (Fig. 4F). Taken together, these results demonstrate that WA selective covalently binds to the Cys47 of PRDX6.

3.5. *WA inhibits the activity of PRDX6 and induces the generation of ROS*

With the covalent binding of WA to PRDX6, we examined the effect of WA on the function of PRDX6 via an enzyme activity assay. As shown in Fig. 5A and Fig. S7A, the enzyme activities of PRDX6 were significantly inhibited by WA and WP. In contrast, WA-1 had a slight inhibitory effect on the enzyme activity of PRDX6 (Fig. 5B). PRDX6 is capable of reducing hydroperoxides through its GPx activity and iPLA2 activity. As shown in Fig. 5C and Fig. S7B, WA and WP remarkably suppressed the GPx activity in H1975 cells, while WA-1 had no significant effect on the GPx activity in H1975 cells (Fig. 5D). Similar results were also shown in the measurement of iPLA2 activity in H1975 cells (Fig. 5E and F and Fig. S7C). Moreover, WA also significantly increased the generation of ROS in H1975 cells (Fig. 5G and H), whereas WA-1 had no obvious effect on the generation of ROS in H1975 cells (Fig. 5I and J). WA also decreased the reduced GSH in H1975 cells (Fig. S7D). Further immunoblotting results showed that the expression of PCNA, Bcl-2, XIAP and survivin regulated by PRDX6 were also decreased after

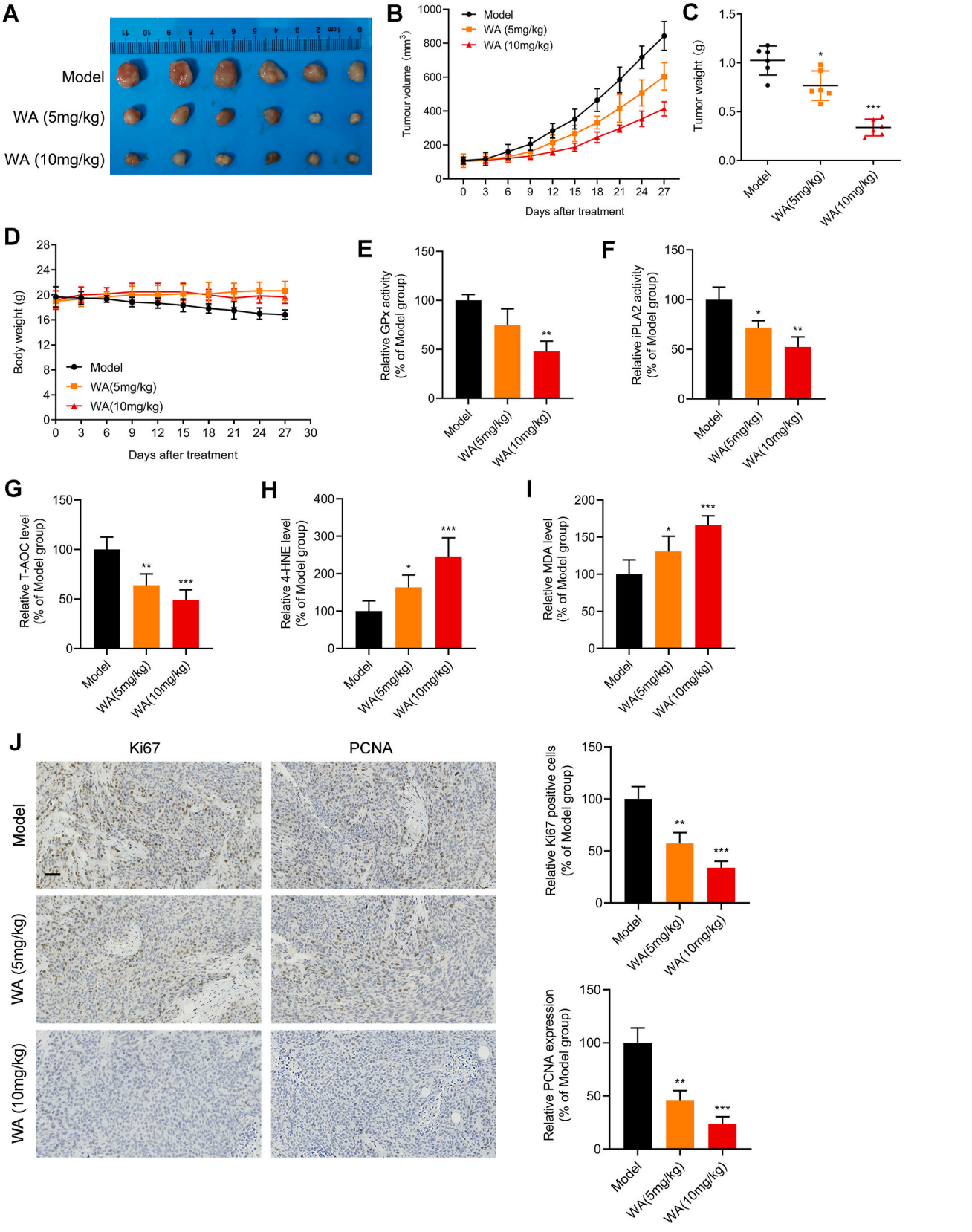

(caption on next page)

Fig. 8. Effect of WA on the proliferation of H1975 non-small cell lung cancer cells in vivo. (A) Tumor images of H1975 cells tumor-bearing mice after treated with WA (5 mg/kg and 10 mg/kg). (B) Changes of tumor volume, (C) tumor weight, and (D) body weight were showed after treated with WA (5 mg/kg and 10 mg/kg) in the xenograft model. Data are presented as the mean ± SD, n = 6, $^{*}P < 0.05$, $^{***}P < 0.001$, compared with model group. (E) GPx activities were measured by a GPx assay kit after treated with WA (5 mg/kg and 10 mg/kg) in tumor tissue. Data are presented as the mean ± SD, n = 6, $^{**}P < 0.01$, compared with model group. (F) iPLA2 activities were measured by an iPLA2 assay kit after treated with WA (5 mg/kg and 10 mg/kg) in tumor tissue. Data are presented as the mean ± SD, n = 6, $^{*}P < 0.05$, $^{**}P < 0.01$, compared with model group. (G) The total antioxidant capacities (T-AOC) in tumor tissue were measured by a total antioxidant assay kit. Data are presented as the mean ± SD, n = 6, $^{**}P < 0.01$, $^{***}P < 0.001$, compared with model group. (H) 4-Hydroxynonenal (4-HNE) were measured by an ELISA assay. Data are presented as the mean ± SD, n = 6, $^{*}P < 0.05$, $^{***}P < 0.001$, compared with model group. (I) The levels of malondialdehyde (MDA) were analyzed by a MDA assay kit. Data are presented as the mean ± SD, n = 6, $^{**}P < 0.01$, $^{***}P < 0.001$, compared with model group. (J) Histopathology of xenograft tumors stained with PCNA and Ki67. Data are presented as the mean ± SD, n = 6, $^{**}P < 0.01$, compared with model group. Scale bar = 50 μm.

treatment of WA (Fig. 5K). Together, these results reveal that WA decreases the activity of PRDX6 and increases the production of ROS in H1975 cells.

3.6. Deficiency of PRDX6 restrains the proliferation and increases the oxidative stress of H1975 cells

In order to assess the function of PRDX6 in H1975 cells, the PRDX6 gene knockout (KO) H1975 cells were generated by CRISPR/Cas9 system. Immunoblotting results showed that PRDX6 was effectively knockout in H1975 cells (Fig. 6A). The deletion of PRDX6 markedly inhibited the proliferation of H1975 cells (Fig. 6B and C).

As a result of the deficiency of PRDX6, the GPx activity and iPLA2 activity were decreased in PRDX6 KO H1975 cells (Fig. 6D and E). In addition, the ROS levels were also increased in PRDX6 KO H1975 cells (Fig. 6F and G). The immunoblotting analysis further showed that the expression of PCNA, Bcl-2, XIAP and survivin were observably decreased in PRDX6 KO H1975 cells (Fig. 6H). Overall, these results indicate that the deficiency of PRDX6 could raise the levels of ROS and inhibit the proliferation of H1975 cells.

3.7. WA-mediated cytotoxicity and generation of ROS are dependent on PRDX6 in H1975 cells

Since PRDX6 was vital to the regulation of ROS and WA could selective covalently bind to PRDX6, we further examined the effect of WA on the proliferation and oxidative stress in PRDX6 KO H1975 cells. Interestingly, in comparison with the control group, PRDX6 KO H1975 cells were insensitive to the treatment of WA (Fig. 7A and B). Notably, WA had no significant inhibition on the GPx and iPLA2 activities in PRDX6 KO H1975 cells (Fig. 7C and D). Furthermore, the ROS levels had no remarkably increased in PRDX6 KO H1975 cells after treatment of WA (Fig. 7E and F). Consistent with these, WA had no obvious effect on the expression of PCNA, Bcl-2, XIAP and survivin in PRDX6 KO H1975 cells (Fig. 7G). In addition, WA had lower cytotoxicity in normal lung epithelial BEAS-2B cells (Fig. S7E), which had lower expression of PRDX6 compared with H1975 cells (Fig. S7F). In summary, these results suggest that PRDX6 contributes to the production of ROS and cytotoxicity mediated by WA in H1975 cells.

3.8. WA suppresses the proliferation of H1975 cells in vivo

To investigate the effect of WA on the proliferation of H1975 cells in vivo, we established a xenograft model of H1975 cells. Compared with the model group, WA dramatically suppressed the growth of tumors (Fig. 8A–C). As shown in Fig. 8D and Fig. S8, WA did not cause an obvious change in the mice body weight, and no obvious morphological changes were observed in the organs of the mice after treating with WA, indicating WA had low toxicity to the mice. Consistent with the results in vitro, WA also inhibited the GPx and iPLA2 activities in the xenograft model of H1975 cells (Fig. 8E and F). As a result of the inhibition of the GPx and iPLA2 activities, the total antioxidant capacity (TAC) was reduced after treatment of WA (Fig. 8G). Meanwhile, the levels of malondialdehyde (MDA) and 4-hydroxynonenal (4HNE), two major lipid peroxidation products, were elevated after treatment of WA (Fig. 8H and I). The positive expression of Ki67 and PCNA were also decreased after the treatment of WA (Fig. 8J). Together, these data indicate that WA could induce the oxidative stress and inhibit the proliferation of H1975 cells in vivo.

3.9. PRDX6 contributes to the inhibition of WA on the proliferation of H1975 cells in vivo

To further evaluate the selectivity of WA on the inhibition of PRDX6, we established a xenograft model of PRDX6 KO H1975 cells. As shown in Fig. 9A–C, the proliferation of PRDX6 KO H1975 cells was slower than the PRDX6 WT H1975 cells in the xenograft model. The positive expression of Ki67 was also significantly decreased in the xenograft model of PRDX6 KO H1975 cells (Fig. 9D). Moreover, the GPx and iPLA2 activities were also decreased in the xenograft model of PRDX6 KO H1975 cells (Fig. 9E and F). Notably, WA had no obvious inhibitory effect on the cell proliferation in the xenograft model of PRDX6 KO H1975 cells (Fig. 9G–I). In addition, there were no remarkable decrease of the GPx and iPLA2 activities after treatment of WA in the xenograft model of PRDX6 KO H1975 cells (Fig. 9J and K). In summary, these results reveal that the inhibition of WA on the proliferation of H1975 cells was dependent on the suppression of PRDX6.

4. Discussion

PRDX6, as an antioxidant enzyme, could reduce cellular peroxides including short chain hydroperoxides and phospholipid hydroperoxides through its GPx activity, which could protect cells against oxidative stress [2,3,7]. There had been reported that inhibition or deficiency of PRDX6 could increase the intracellular oxidative stress and cause the cell injury [39–41]. Increasing evidence had demonstrated that PRDX6 had a critical role in the development of human cancers [19,23]. High levels of PRDX6 has been found in multiple cancer cells and contributes to the proliferation of cancer cells. Therefore, selective inhibition of PRDX6 provides a potential therapeutic strategy for certain cancers with overexpressed PRDX6. Nonetheless, only a few inhibitors of PRDX6 have been discovered to date, which is limited to the development of targeting PRDX6 therapeutic strategy in cancer.

Here, we firstly report that WA, a natural small molecule, is a novel covalent inhibitor of PRDX6. Currently, the reported PRDX6 inhibitors are mostly competitive inhibitors [42,43], whereas no covalent inhibitors of PRDX6 have been reported to date. Although there had been reported that thiacremonone could bind to PRDX6, whereas there was no direct evidence to support the covalent binding of PRDX6 and thiacremonone [43]. In this study, we designed and synthesized an alkyne-tagged WA-based active probe WP to identify the direct target of WA. With the utilization of SILAC-ABPP, we discovered that WA could directly bind to PRDX6 and inhibit the activity of PRDX6.

Due to the α, β-unsaturated ketone moiety is considered as a Michael acceptor that could covalently bind to the thiol of cysteine in protein. We speculated whether WA is bound to PRDX6 by the α, β-unsaturated ketone moiety. Interestingly, WA-1 had no obvious influence on the proliferation of H1975 cells, which had a reduced α, β-unsaturated ketone moiety. There was almost no interaction between WA-1 and PRDX6 in the BLI assay. Since the dependency of GPx and iPLA2 activities on

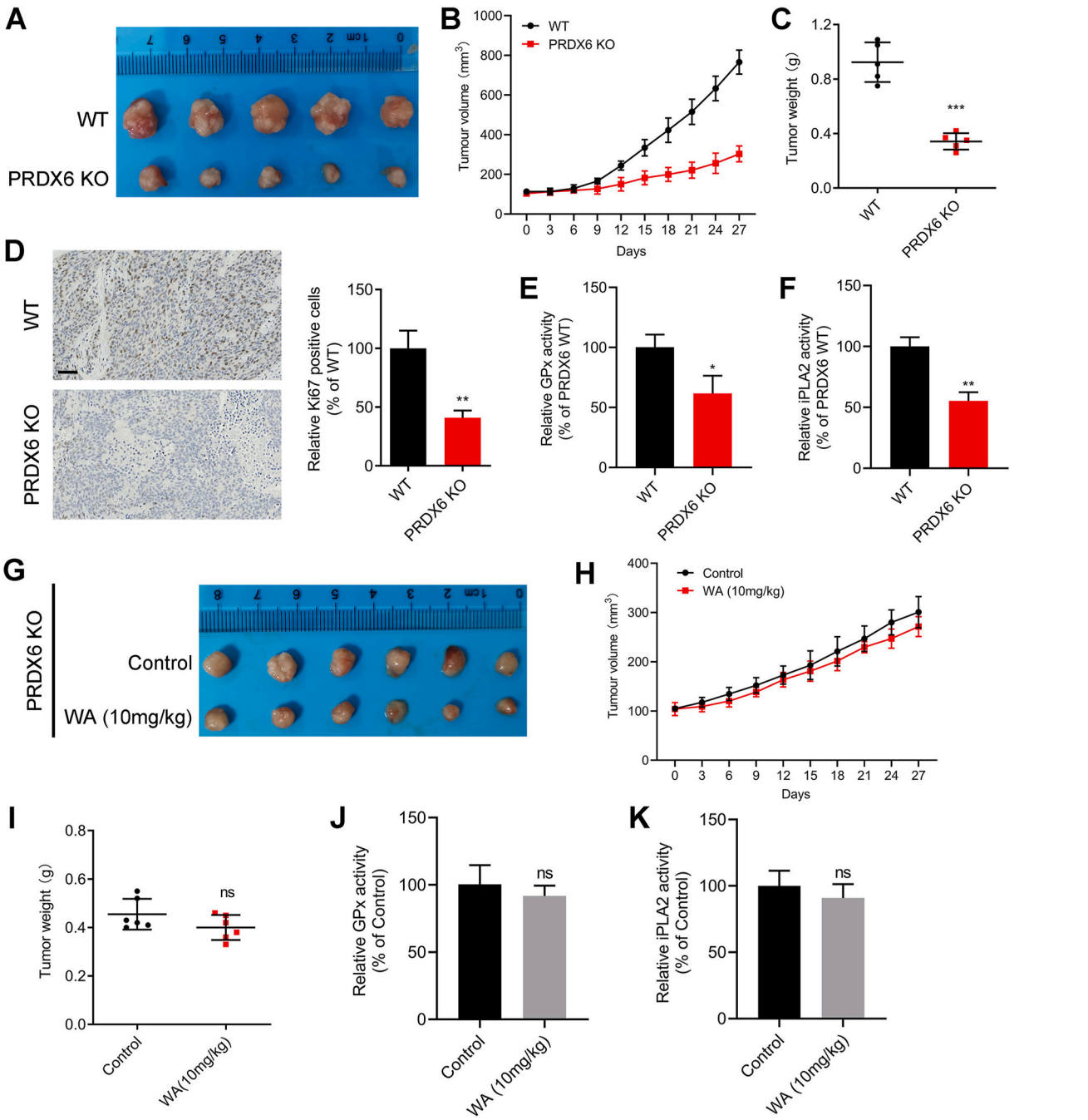

Fig. 9. Effect of WA on the proliferation of PRDX6 KO H1975 cells in vivo. (A) Tumor images of PRDX6 WT and PRDX6 KO H1975 cells in xenograft model. (B) Changes of tumor volume were showed in xenograft model of PRDX6 WT and PRDX6 KO H1975 cells. (C) Tumor weight of PRDX6 WT and PRDX6 KO H1975 cells in xenograft model. Data are presented as the mean ± SD, n = 6, $^{***}P < 0.001$, compared with WT group. (D) Histopathology of xenograft tumors stained with Ki67. Data are presented as the mean ± SD, n = 6, $^{**}P < 0.01$, compared with WT group. Scale bar = 50 μm. (E) GPx activities were measured by a GPx assay kits in xenograft model of PRDX6 WT and PRDX6 KO H1975 cells. Data are presented as the mean ± SD, n = 6, $^{*}P < 0.05$, compared with WT group. (F) iPLA2 activities were measured by an iPLA2 assay kits in xenograft model of PRDX6 WT and PRDX6 KO H1975 cells. Data are presented as the mean ± SD, n = 6, $^{**}P < 0.01$, compared with WT group. (G) Tumor images of PRDX6 KO H1975 cells tumor-bearing mice after treated with WA (10 mg/kg). (H) Changes of tumor volume, (I) tumor weight were showed after treated with WA (10 mg/kg) in xenograft model of PRDX6 KO H1975 cells. Data are presented as the mean ± SD, n = 6, ns, no significance, compared with control group. (J) GPx activities and (K) iPLA2 activities were measured by a GPx assay kits and a iPLA2 assay kits after treated with WA (10 mg/kg) in xenograft model of PRDX6 KO H1975 cells. Data are presented as the mean ± SD, n = 6, ns, no significance, compared with control group.

PRDX6, the enzyme activity inhibition of PRDX6 by WA also effectively restrained the GPx and iPLA2 activities in H1975 cells. However, WA-1 almost did not affect the GPx and iPLA2 activities, further supporting the inhibition of PRDX6 by WA was dependent on the α, β-unsaturated ketone moiety.

PRDX6 is a bifunctional protein with both the GPx and iPLA2 activities, which could reduce the lipid peroxidation products such as malondialdehyde (MDA) and 4-hydroxynonenal (4-HNE) [7]. There had been reported that 4-HNE, an a,β-unsaturated aldehydes, could covalently modify to the Cys47 and Cys91 of PRDX6, which provided additional evidence for explaining the partial loss of PRDX6 activity upon 4-HNE treatment [44,45]. In the present study, no potential

modification of 4-HNE was identified on PRDX6 in the LC-MS/MS results. Therefore, the a,β-unsaturated aldehydes may not involved in the inhibition of PRDX6 by WA in the present study.

In the reported study [23], knockout of PRDX6 by CRISPR/Cas9 system had an antiproliferative effect in tumor cells. In the present study, we also screened the viable cell which had the deletion of PRDX6 by CRISPR/Cas9 system. The proliferation of PRDX6 KO H1975 cells was slower than the PRDX6 WT H1975 cells (Fig. 6B and C). The ROS level of PRDX6 WT H1975 cells was also higher than that in PRDX6 KO H1975 cells (Fig. 6F and G). The inhibition of PRDX6 by WA could lead to the accumulation of hydrogen peroxide and phospholipid hydroperoxides, which elevated the intracellular oxidative stress and caused cell injury. Therefore, the elevated oxidative stress mainly contributed to the proliferation inhibition of H1975 cells by WA.

Unlike the other PRDXs, PRDX6 is the sole 1-Cys PRDXs. The cysteine at position 47 (Cys47) in the amino acid sequence of PRDX6 is the active site for the GPx activity [1,7]. Mutation of PRDX6 at Cys47 could result in the inactivation of PRDX6 [2]. In this study, the LC-MS/MS analysis further demonstrated that WA was covalently bound to the Cys47 residue of PRDX6 while not the Cys91. Furthermore, the point mutation also showed that WA had no interaction with the recombinant Cys47A protein and the Cys47A mutated Flag-PRDX6. Although thiacremonone was also reported to bind to the Cys47 of PRDX6, there was no direct evidence for the binding of thiacremonone to the Cys47 of PRDX6. Therefore, WA was the first reported covalent inhibitor of PRDX6 to date.

Collectively, our findings reveal that WA is the first PRDX6 covalent inhibitor, which could serve as a promising lead compound in the development of new therapeutic agents for PRDX6-dependent cancers, and also provides a novel chemical tool to investigate the functions of PRDX6.

Author contributions

Lingyi Kong and Jianguang Luo initiated and supervised the research. Chen Chen designed and performed the experiments, interpreted the data, and drafted the manuscript. Tianyu Zhu designed the chemical synthesis strategy and interpreted the compound data. Xiaoqin Liu and Lijie gong performed partial cellular assays. Wuxi zhou extracted and purified the research reagents.

Declaration of competing interest

The authors declare no conflicts of interest.

Acknowledgments

This work was supported by the National Natural Science Foundation of China (81872983, 81903861), the Natural Science Foundation of Jiangsu Province (BK20181329), and the Program for Changjiang Scholars and Innovative Research Team in University (IRT_15R63).

Appendix A. Supplementary data

Supplementary data to this article can be found online at https://doi.org/10.1016/j.redox.2021.102130.

References

[1] H. Li, B. Benipal, S. Zhou, C. Dodia, S. Chatterjee, J.Q. Tao, E.M. Sorokina, T. Raabe, S.I. Feinstein, A.B. Fisher, Critical role of peroxiredoxin 6 in the repair of peroxidized cell membranes following oxidative stress, Free Radic. Biol. Med. 87 (2015) 356–365.
[2] A.B. Fisher, Peroxiredoxin 6: a bifunctional enzyme with glutathione peroxidase and phospholipase a2 activities, Antioxidants Redox Signal. 15 (2011) 831–844.
[3] A.B. Fisher, Antioxidants special issue: peroxiredoxin 6 as a unique member of the peroxiredoxin family, Antioxidants 8 (2019) 5–9.
[4] S.I. Feinstein, Mouse models of genetically altered peroxiredoxin 6, Antioxidants 8 (2019) 1–10.
[5] Y. Manevich, T. Shuvaeva, C. Dodia, A. Kazi, S.I. Feinstein, A.B. Fisher, Binding of peroxiredoxin 6 to substrate determines differential phospholipid hydroperoxide peroxidase and phospholipase A2 activities, Arch. Biochem. Biophys. 485 (2009) 139–149.
[6] Y. Manevich, K.S. Reddy, T. Shuvaeva, S.I. Feinstein, A.B. Fisher, Structure and phospholipase function of peroxiredoxin 6: identification of the catalytic triad and its role in phospholipid substrate binding, J. Lipid Res. 48 (2007) 2306–2318.
[7] J.A. Arevalo, J.P. Vázquez-Medina, The role of peroxiredoxin 6 in cell signaling, Antioxidants 7 (2018).
[8] A.B. Fisher, J.P. Vasquez-Medina, C. Dodia, E.M. Sorokina, J.Q. Tao, S.I. Feinstein, Peroxiredoxin 6 phospholipid hydroperoxidase activity in the repair of peroxidized cell membranes, Redox Biol. 14 (2018) 41–46.
[9] A.B. Fisher, Peroxiredoxin 6 in the repair of peroxidized cell membranes and cell signaling, Arch. Biochem. Biophys. 617 (2017) 68–83.
[10] J.W. Chen, C. Dodia, S.I. Feinstein, M.K. Jain, A.B. Fisher, 1-Cys peroxiredoxin, a bifunctional enzyme with glutathione peroxidase and phospholipase A2 activities, J. Biol. Chem. 275 (2000) 28421–28427.
[11] Y. Manevich, A.B. Fisher, Peroxiredoxin 6, a 1-Cys peroxiredoxin, functions in antioxidant defense and lung phospholipid metabolism, Free Radic. Biol. Med. 38 (2005) 1422–1432.
[12] T.J. Nevalainen, 1-Cysteine peroxiredoxin: a dual-function enzyme with peroxidase and acidic Ca2+-independent phospholipase A2 activities, Biochimie 92 (2010) 638–644.
[13] X.Z. Chang, D.Q. Li, Y.F. Hou, J. Wu, J.S. Lu, G.H. Di, W. Jin, Z.L. Ou, Z.Z. Shen, Z. M. Shao, Identification of the functional role of peroxiredoxin 6 in the progression of breast cancer, Breast Cancer Res. 9 (2007) 1–15.
[14] M. Jo, H.M. Yun, K.R. Park, M. Hee Park, T. Myoung Kim, J. Ho Pak, S. Jae Lee, D. C. Moon, C.W. Park, S. Song, C.K. Lee, S. Bae Han, J. Tae Hong, Lung tumor growth-promoting function of peroxiredoxin 6, Free Radic. Biol. Med. 61 (2013) 453–463.
[15] X. Hu, E. Lu, C. Pan, Y. Xu, X. Zhu, Overexpression and biological function of PRDX6 in human cervical cancer, J. Canc. 11 (2020) 2390–2400.
[16] J.H. Pak, W.H. Choi, H.M. Lee, W.D. Joo, J.H. Kim, Y.T. Kim, Y.M. Kim, J.H. Nam, Peroxiredoxin 6 overexpression attenuates cisplatin-induced apoptosis in human ovarian cancer cells, Canc. Invest. 29 (2011) 21–28.
[17] L.G.M. José, T.V.R. María, C.H. Beatriz, L.R. Daniel, P. José, M. Brian, R.A. Raquel, B.J. Antonio, P.C. Alicia, Peroxiredoxin 6 down-regulation induces metabolic remodeling and cell cycle arrest in HepG2 cells, Antioxidants 8 (2019) 1–17.
[18] B. Walsh, A. Pearl, S. Suchy, J. Tartaglio, K. Visco, S.A. Phelan, Overexpression of Prdx6 and resistance to peroxide-induced death in Hepa1-6 cells: Prdx suppression increases apoptosis, Redox Rep. 14 (2009) 275–284.
[19] H.M. Yun, K.R. Park, H.P. Lee, D.H. Lee, M. Jo, D.H. Shin, D.Y. Yoon, S.B. Han, J. T. Hong, PRDX6 promotes lung tumor progression via its GPx and iPLA2 activities, Free Radic. Biol. Med. 69 (2014) 367–376.
[20] H.M. Yun, K.R. Park, M.H. Park, D.H. Kim, M.R. Jo, J.Y. Kim, E.C. Kim, D.Y. Yoon, S.B. Han, J.T. Hong, PRDX6 promotes tumor development via the JAK2/STAT3 pathway in a urethane-induced lung tumor model, Free Radic. Biol. Med. 80 (2015) 136–144.
[21] J. Xu, Q. Su, M. Gao, Q. Liang, J. Li, X. Chen, Differential expression and effects of peroxiredoxin-6 on drug resistance and cancer stem cell-like properties in non-small cell lung cancer, OncoTargets Ther. 12 (2019) 10477–10486.
[22] N. Sahu, J.P. Stephan, D. Dela Cruz, M. Merchant, B. Haley, R. Bourgon, M. Classon, J. Settleman, Functional screening implicates miR-371-3p and peroxiredoxin 6 in reversible tolerance to cancer drugs, Nat. Commun. 7 (2016) 1–10.
[23] M.J. López-Grueso, D.J. Lagal, Á.F. García-Jiménez, R.M. Tarradas, B. Carmona-Hidalgo, J. Peinado, R. Requejo-Aguilar, J.A. Bárcena, C.A. Padilla, Knockout of PRDX6 induces mitochondrial dysfunction and cell cycle arrest at G2/M in HepG2 hepatocarcinoma cells, Redox Biol. 37 (2020).
[24] T. Ma, W.N. Zhang, L. Yang, C. Zhang, R. Lin, S.M. Shan, M. Di Zhu, J.G. Luo, L. Y. Kong, Cytotoxic withanolides from: Physalis angulata var. villosa and the apoptosis-inducing effect via ROS generation and the activation of MAPK in human osteosarcoma cells, RSC Adv. 6 (2016) 53089–53100.
[25] S. Pan, S.Y. Jang, D. Wang, S.S. Liew, Z. Li, J.S. Lee, S.Q. Yao, A suite of "minimalist" photo-crosslinkers for live-cell imaging and chemical proteomics: case study with BRD4 inhibitors, Angew. Chem. Int. Ed. 56 (2017) 11816–11821.
[26] T. Kambe, B.E. Correia, M.J. Niphakis, B.F. Cravatt, Mapping the protein interaction landscape for fully functionalized small-molecule probes in human cells, J. Am. Chem. Soc. 136 (2014) 10777–10782.
[27] L.C. Wang, L.X. Liao, H.N. Lv, D. Liu, W. Dong, J. Zhu, J.F. Chen, M.L. Shi, G. Fu, X. M. Song, Y. Jiang, K.W. Zeng, P.F. Tu, Highly selective activation of heat shock protein 70 by allosteric regulation provides an insight into efficient neuroinflammation inhibition, EBioMedicine 23 (2017) 160–172.
[28] S. Zhou, E.M. Sorokina, S. Harper, H. Li, L. Ralat, C. Dodia, D.W. Speicher, S. I. Feinstein, A.B. Fisher, Peroxiredoxin 6 homodimerization and heterodimerization with glutathione S-transferase pi are required for its peroxidase but not phospholipase A2 activity, Free Radic. Biol. Med. 94 (2016) 145–156.
[29] T. Ma, Y. Zhang, C. Zhang, J.G. Luo, L.Y. Kong, Downregulation of TIGAR sensitizes the antitumor effect of physapubenolide through increasing intracellular ROS levels to trigger apoptosis and autophagosome formation in human breast carcinoma cells, Biochem. Pharmacol. 143 (2017) 90–106.
[30] A. Devarajan, N.S. Rajasekaran, C. Valburg, E. Ganapathy, S. Bindra, W.A. Freije, Maternal perinatal calorie restriction temporally regulates the hepatic autophagy and redox status in male rat, Free Radic. Biol. Med. 130 (2019) 592–600.

[31] S.Q. Wang, X.Y. Yang, S.X. Cui, Z.H. Gao, X.J. Qu, Heterozygous knockout insulin-like growth factor-1 receptor (IGF-1R) regulates mitochondrial functions and prevents colitis and colorectal cancer, Free Radic. Biol. Med. 134 (2019) 87–98.
[32] S. Pan, H. Zhang, C. Wang, S.C.L. Yao, S.Q. Yao, Target identification of natural products and bioactive compounds using affinity-based probes, Nat. Prod. Rep. 33 (2016) 612–620.
[33] R. Lonsdale, R.A. Ward, Structure-based design of targeted covalent inhibitors, Chem. Soc. Rev. 47 (2018) 3816–3830.
[34] M.H. Wright, S.A. Sieber, Chemical proteomics approaches for identifying the cellular targets of natural products, Nat. Prod. Rep. 33 (2016) 681–708.
[35] J. Wang, L. Gao, Y.M. Lee, K.A. Kalesh, Y.S. Ong, J. Lim, J.E. Jee, H. Sun, S.S. Lee, Z.C. Hua, Q. Lin, Target identification of natural and traditional medicines with quantitative chemical proteomics approaches, Pharmacol. Ther. 162 (2016) 10–22.
[36] C. Wang, S. Li, J. Zhao, H. Yang, F. Yin, M. Ding, J. Luo, X. Wang, L. Kong, Design and SAR of Withangulatin A analogues that act as covalent TrxR inhibitors through the Michael addition reaction showing potential in cancer treatment, J. Med. Chem. 63 (2020) 11195–11214.
[37] M. Gersch, J. Kreuzer, S.A. Sieber, Electrophilic natural products and their biological targets, Nat. Prod. Rep. 29 (2012) 659–682.
[38] A.J. Maurais, E. Weerapana, Reactive-cysteine profiling for drug discovery, Curr. Opin. Chem. Biol. 50 (2019) 29–36.
[39] R. Arriga, F. Pacifici, B. Capuani, A. Coppola, A. Orlandi, M.G. Scioli, D. Pastore, A. Andreadi, P. Sbraccia, M. Tesauro, N. Di Daniele, G. Sconocchia, G. Donadel, A. Bellia, D. Della-Morte, D. Lauro, Peroxiredoxin 6 is a key antioxidant enzyme in modulating the link between glycemic and lipogenic metabolism, Oxid. Med. Cell. Longev. 2019 (2019).
[40] Y.K. So, H.Y. Jo, H.K. Mi, Y.Y. Cha, W.C. Sung, J.H. Shim, J.K. Tae, K.Y. Lee, H2O2-dependent hyperoxidation of peroxiredoxin 6 (Prdx6) plays a role in cellular toxicity via up-regulation of iPLA2 activity, J. Biol. Chem. 283 (2008) 33563–33568.
[41] N. Fatma, P. Singh, B. Chhunchha, E. Kubo, T. Shinohara, B. Bhargavan, D. P. Singh, Deficiency of Prdx6 in lens epithelial cells induces ER stress response-mediated impaired homeostasis and apoptosis, Am. J. Physiol. Cell Physiol. 301 (2011) 954–967.
[42] H.L. Lee, M.H. Park, D.J. Son, H.S. Song, J.H. Kim, S.C. Ko, M.J. Song, W.H. Lee, J. H. Yoon, Y.W. Ham, S.B. Han, J.T. Hong, Anti-cancer effect of snake venom toxin through down regulation of AP-1 mediated PRDX6 expression, Oncotarget 6 (2015) 22139–22151.
[43] M. Jo, H.M. Yun, K.R. Park, M.H. Park, D.H. Lee, S.H. Cho, H.S. Yoo, Y.M. Lee, H. S. Jeong, Y. Kim, J.K. Jung, B.Y. Hwang, M.K. Lee, N.D. Kim, S.B. Han, J.T. Hong, Anti-cancer effect of thiacremonone through down regulation of peroxiredoxin 6, PLoS One 9 (2014) 1–10.
[44] Y. Chen, Y. Cong, B. Quan, T. Lan, X. Chu, Z. Ye, X. Hou, C. Wang, Chemoproteomic profiling of targets of lipid-derived electrophiles by bioorthogonal aminooxy probe, Redox Biol. 12 (2017) 712–718.
[45] J.R. Roede, D.L. Carbone, J.A. Doorn, O.V. Kirichenko, P. Reigan, D.R. Petersen, In vitro and in silico characterization of peroxiredoxin 6 modified by 4-hydroxynonenal and 4-oxononenal, Chem. Res. Toxicol. 21 (2008) 2289–2299.